Anal Bioanal Chem (2010) 398:751–758
DOI 10.1007/s00216-010-3994-z

ORIGINAL PAPER

Evaluation of nucleic acid duplex formation on gold over layers in biosensor fabricated using Czochralski-grown single-crystal silicon substrate

Subash C. B. Gopinath · Ramanujam Kumaresan · Koichi Awazu · Makoto Fujimaki · Minoru Mizuhata · Junji Tominaga · Penmetcha K. R. Kumar

Received: 13 May 2010 / Revised: 29 June 2010 / Accepted: 30 June 2010 / Published online: 14 July 2010

Abstract With a view to developing an economical and elegant biosensor chip, we compared the efficiencies of biosensors that use gold-coated single-crystal silicon and amorphous glass substrates. The reflectivity of light over a wide range of wavelengths was higher from gold layer coated single-crystal silicon substrates than from glass substrates. Furthermore, the efficiency of reflection from gold layers of two different thicknesses was examined. The thicker gold layer (100 nm) on the single-crystal silicon showed a higher reflectivity than the thinner gold film (10 nm). The formation of a nucleic acid duplex and aptamer–ligand interactions were evaluated on these gold layers, and a crystalline silicon substrate coated with the 100-nm-thick gold layer is proposed as an alternative substrate for studies of interactions of biomolecules.

Keywords Spectrophotometry · Crystal · Amorphous · Au layer · DNA hybridization

Electronic supplementary material The online version of this article (doi:10.1007/s00216-010-3994-z) contains supplementary material, which is available to authorized users.

S. C. B. Gopinath (✉) · K. Awazu · M. Fujimaki
Photonics Research Institute, National Institute of Advanced Industrial Science and Technology (AIST),
1-1-1 Higashi,
Tsukuba, Ibaraki 305-8562, Japan
e-mail: gopi-subashchandrabose@aist.go.jp

R. Kumaresan · M. Mizuhata
Department of Chemical Science and Engineering,
Graduate School of Engineering, Kobe University,
Kobe 657-8501, Japan

S. C. B. Gopinath · J. Tominaga
Nanodevice Innovation Research Center, AIST,
1-1-1 Higashi,
Tsukuba, Ibaraki 305-8562, Japan

P. K. R. Kumar
Biomedical Research Institute, AIST,
1-1-1 Higashi,
Tsukuba, Ibaraki 305-8566, Japan

Introduction

A biosensor is a device that permits investigators to detect extremely small amounts of chemical or biochemical agents in a biological medium. Research to reduce the size and increase the reliability of biosensors will revolutionize the field of biomedical measurements. Development of chips for sensing various materials is vital in the field of nanobiotechnology, especially in biosensor development. In the field of nanobiotechnology, several detection systems have been developed for the measurement of minute quantities of biomolecules by "top-down" and "bottom-up" approaches [1]. Among the sensor surfaces that have been developed are nanoscale biosensors with gold (Au) surfaces that use thiolated biomolecules as linkers [2–6]. The use of Au surfaces capable of screening libraries of drugs or inhibitors on spinning-disk systems such as the BioCD and the BioDVD is an emerging technology [7–11]. Sensors on silicon or silica substrates are also widely used in the analysis of interactions of biomolecules [12–16]. Because of their nature, these substrates provide a variation in the degree of packing and, consequently, variations in the densities, thicknesses, and morphologies of the deposited films [17]. An optical property, such as light reflectivity, of a single-crystal silicon-based sensor is different from that of an amorphous glass substrate. Light reflections on this kind

of sensor substrate are changes in the direction of a wavefront at an interface between two different media which leads the wavefront to returns into the medium from which it originated. Reflections are sensitive to a tiny refractive index change on the deposited thin gold film. Once a molecule binds to the surface, there will be changes in the reflectivity due to refractive index changes. In the present study, the reflection changes were monitored on materials prepared by Czochralski technique which is a conventionally used crystal growth method for the growth of single-crystal ingots, especially silicon (Electronic Supplementary Material figure S1a).

Currently, several sensor chips for conventional methods are available; these have low detection limits, but are expensive and time-consuming, and require highly trained personnel. It is in vogue to develop biosensors as new analytical tools capable of providing rapid and reliable measurements at low cost [18]. Performance specifications for sensor chips include accuracy and long-term stability, coupled with a small size. Keeping these criteria in mind, we prepared a chip from silicon with a deposited Au layer that has a small size and a low cost, and is capable of detecting the formation of nucleic acid duplexes; this Au-coated silicon can serve as an alternative substrate for the development of sensors. Furthermore, we have shown that these chips are suitable for monitoring interactions of biomolecules when used in conjunction with commonly available spectrophotometric techniques. Using the strategy of reflection changes on solid surface upon attaching biomolecules are explained with gold thin film deposited on the silicon substrate.

Materials and methods

Oligonucleotides

A 5′-thiolated DNA consisting of 20 deoxythiamine residues (dT_{20}) with protected thiolated groups was prepared chemically. To deprotect the thiolated groups, the oligonucleotide were treated with dithiothreitol (DTT, 60 mM) in Tris–HCl buffer (250 mM, pH 8.0) for 16 h at room temperature. After the reaction, the SH-poly-dT_{20} oligonucleotide was purified by passage through an ODS-120 T column [Tosoh, Japan; TSK-gel, size 7.8 mm (internal diameter)×30.0 cm long] in an HPLC system (Shimadzu, Japan) run with 2.5 mM triethylammonium acetate (TEAA) at 5.0 MPa pressure, and eluted with a linear concentration of TEAA and acetonitrile at a ratio of 60:40 and a flow rate of 2 mL/min. All fractions were monitored spectrophotometrically at a wavelength of 254 nm. The solution corresponding to the peak area was collected and dialyzed twice against double-distilled water for 2 h each time. The dialyzed sample was concentrated to dryness in vacuum, and the concentration of DNA was measured. Commercially available oligomers were used to analyze the formation of a DNA duplex (thiol dT_{20}–dA_{20}) and the formation of noncomplementary products with dT_{20}.

A 33-mer stable RNA-aptamer, previously selected against factor IXa [19], was enzymatically synthesized by in vitro transcription, using T7 RNA polymerase on a synthetic DNA template. The template with the T7 promoter region (in italics; 5′-*AGTAATACGACTCACTA-TAGG*GATGGGGACTATACCGCGTAATGCTG-3′) was synthesized to generate the double-stranded DNA. Using this template DNA and the primers (forward 5′-AGTAA-TACGACTCACTATAGG-3′; reverse 5′-$(T)_{24}$ATGGG-GAGGCAGCATTACGCGGTATA-3′), a PCR reaction was performed with a commercial PCR kit (Ex *Taq* kit, Takara, Japan). The reaction mixture was cycled at 94 °C for 70 s, 55 °C for 50 s, and 72 °C for 70 s for 15 cycles. The PCR product was precipitated and used for RNA preparation by in vitro T7 transcription. Transcription was performed at 37 °C overnight, with a DuraScribe transcription kit (Epicentre Biotechnologies, USA). Afterwards, the products were treated with 2 U of DNase I (RNase free) for 10 min at 37 °C, to remove the template DNA, and were mixed with an equal volume of 2× urea buffer (7 M urea, 50 mM EDTA, 90 mM Tris–borate containing 0.05% bromophenol blue). The reaction mixtures were denatured at 90 °C for 2 min and fractionated on a 15% polyacrylamide gel containing 7 M urea. The RNA band was excised, and the RNA was eluted from the gel. The RNAs were vacuum-concentrated, re-dissolved in water, and then quantitated by the absorbance at 260 nm. The resulting transcribed RNA (57-mer) had 33 nucleotides (which specifically recognize human factor IXa) and 24 nucleotides of A residues at its 5′- and 3′-ends, respectively.

Fabrication of silicon substrates

The silicon substrate was prepared from a Si wafer obtained from a single-crystal silicon ingot. Chips measuring 8× 8 mm (64 mm^2 in area) were cut from the silicon wafer. The wafers were chemo-mechanically polished, and the chips were thoroughly cleaned by the SPM cleaning process [20], before the Au thin layer was formed. The thin films of gold (Au) or platinum (Pt) were fabricated on the cleaned silicon substrates by thermal evaporation. By using an in situ crystal-thickness monitor, the thickness of the thin film was controlled to be 10 or 100 nm. The metal-coated substrates were used for the fabrication of biosensor chips. The suitability of surfaces for fabrication of biosensor was observed using a scanning electron microscope (JEOL JSM-6335 F).

Signal readout by UV spectrophotometer

An ultraviolet–visible–near-infrared (UV–vis–NIR) recording spectrophotometer (Shimadzu UV-3100) was used to examine the spectral changes associated with the binding of partner molecules by monitoring changes in reflectivity over the wavelength range from 350 to 1250 nm. The baseline was adjusted and measured after spotting of each molecule. The reflection mode was set and nullified with a basic signal. Measurements were manipulated by calculation as suggested previously [21], and data manipulation was performed by using a Microsoft Excel spreadsheet.

Analysis of formation of nucleic acid duplexes

Gold-coated silicon substrates, as described above, were used to evaluate the formation of DNA duplexes. As an initial step, 100 μl of DNA carrying 20 thymine molecules linked to thiol molecules were spotted manually on the chip at a concentration of 1 μM [dissolved in a 100 mM aqueous solution of (2-[4-(2-hydroxyethyl)piperazin-1-yl]ethanesulfonic acid (HEPES) and KOH (pH 7.4) and 50 mM NaCl], and then left for 1 h to achieve proper attachment. The chips were washed thoroughly with the same buffer. After washing, the chip was dried under nitrogen gas with an air gun and the reflectivity was measured on the scanning UV–vis–NIR spectrophotometer. Noncomplementary DNA (dT_{20}) was attached at a similar concentration to the chip with the immobilized thiol-dT_{20} and left for 10 min. The chip was washed with buffer and dried as described above, and then measurements were taken. Complementary reactions were similarly performed with dA_{20}. Similarly, RNA-aptamer was also attached to analyze their interaction with factor IX. For these interactive analyses similar buffer and loading conditions were used as mentioned above, however, 5 mM $CaCl_2$ and $MgCl_2$ were added to the buffer for specific interactions of aptamer and factor IX.

Analysis of biomolecular interactions by surface plasmon resonance

To check the specificity of DNA duplex formation, we conducted experiments using the surface plasmon resonance (SPR) method on Biacore 2000, with a Au-layered sensor chip (Biacore, Sweden). The thiolated DNA (dT_{20}) was immobilized on the Au layer and the formation of complementary and noncomplementary complexes was monitored. After the attachment of the thiolated DNA at a concentration of 1 μM, excess or unbound oligomers were washed away with buffer (HEPES KOH, pH 7.4, as provided by manufacturer) at a flow rate of 2 μL/min for 10 min. To evaluate duplex formation, complementary DNA (dA_{20}) was injected at a flow rate of 2 μL/min for 10 min. Similarly, for the noncomplementary negative reaction, dT_{20} was injected at a similar flow rate into another flow cell on the chip.

Similarly, on a streptravidin-coated sensor chip, from Biacore, Sweden, the interactions of RNA-aptamer and factor IX were evaluated for specific and non-specific in the presence and absence of calcium and magnesium ions in the buffer. To determine the binding affinity of the aptamer, we prepared the aptamer with 24-mer poly(A) nucleotides at the 3′-end, which could anneal to the complementary biotinylated oligo(dT) (5′-biotin-$(T)_{24}$-3′). To prepare this 3′-end extended RNA, we used two primers: a T7 forward primer similar to that used in the above study and a 3′-end primer [5′-$(T)_{24}$-ATGGGGAGGCAGCATTACGCGG-TATA-3′]. The double-stranded DNA template was generated by PCR and transcribed in vitro, as described above. Initially, the biotinylated oligo $(dT)_{24}$ was attached to the streptavidin (SA chip, Biacore, Sweden) by dissolving the oligo dT in binding buffer (5 μM final concentration) and injecting it for 12 to 24 s, to obtain a response of 1,000 resonance units (RU), at a flow rate of 5 μl/min. The excess or unbound biotinylated oligo dT was removed with binding buffer containing 5 mM $CaCl_2$, at a flow rate of 20 μl/min for 10 min. To analyze the binding of the aptamer, 20 μl (50 nM final concentrations) of the aptamer was injected at a flow rate of 2 μl/min for 10 min, which resulted in an increase of about 1,200 RU upon aptamer binding to the complementary biotinylated primer. After each measurement, the sensor chip was washed with a buffer solution, followed by 10 mM NaOH, before the next injection.

Results and discussion

The efficiencies of sensors formed on single-crystal silicon and amorphous glass substrates were examined by using a Czochralski-grown single-crystal silicon wafer and a glass slide as substrates, respectively. Thin Au or Pt layers of thickness 10 or 100 nm were coated on cleaned substrates by means of thermal evaporation. Reflections from these substrates were scanned with a spectrophotometer to examine the reflective properties of the substrate as a function of the wavelength. Reports are available on the applications of spectrophotometric analyses with different format such as, a glass vial [22], a lab-on-a-chip [23], microflow analysis [24], etc. In our study, to reduce the cost of the Au coating on the chips, we reduced the size of the chip to 8×8 mm (area 64 mm^2) to fit within the circular hole on the stage of the spectrophotometer. Because the chip was exactly the same size as the hole in the stage of the spectrophotometer, we used a cover glass between the hole and chip to prevent it from falling through the hole. To

check for any changes in reflection produced by the cover glass, we measured its reflective effect and found that there was no significant change in reflection with the cover glass, and that we could obtain 100% reflection levels within the range 350 to 1550 nm in the presence of a reflective mirror (Electronic Supplementary Material figure S2a and b).

Evaluation of reflections from single-crystal silicon and amorphous glass

In general, the reflectivity of a solid substrate depends on the nature of the substance of which it consists; in the present case, both single-crystal silicon and amorphous glass substrates were used, and their reflection levels were measured. The measurements were made by scanning the chips (coated with Au layer) on a cover glass (Fig. 1a). Both substrates showed high levels of reflection over the range of wavelengths from 350 to 1250 nm. The level of reflection was 65% from single-crystal silicon, and 55% from glass. Even though, the level of reflection was more than 50% in both cases, the single-crystal silicon substrate showed 10% more reflection than did glass (Fig. 1b), possibly as a result of the more orderly structure of the former in comparison with the latter (Electronic Supplementary Material figure S1b). Materials for the fabrication of Au layers were evaluated for their surface uniformity by scanning electron microscopic technique. It was observed that the Au layer on single-crystal silicon exhibited a continuously uniform layer, whereas the Au layer on amorphous glass substrate exhibited the inclusion of cracks, as shown in Fig. 2a and b. Because of this difference in the nature of the materials, the optical reflectivity is higher in case of single-crystal silicon compared to the amorphous glass, in which the present cracks cause the distraction of irradiated light, resulting in the reduction of light reflectance.

When we scanned glass lacking a Au layer, the light was completely transmitted in the absence of the reflective mirror (data not shown). In addition, we also found that, unlike those on single-crystal silicon, Au films deposited on glass were insufficiently robust during the various washing and drying processes required in the analyses. On the basis of these results, single-crystal silicon is a better substrate than glass for use in reflection-based sensors, and we used Czochralski-grown single-crystal silicon substrates in all subsequent experiments. Further, similar studies were performed with single-crystal silicon and amorphous glass coated with Pt, since Pt is also reported to be suitable substrate for biomolecular binding [25]. In this comparative study, in contrast to the Au-coated materials, Pt-coated materials showed nearly equal reflections with single-crystal silicon (~29%) and amorphous glass (~27%; Fig. 1c). These reflection levels were nearly half values

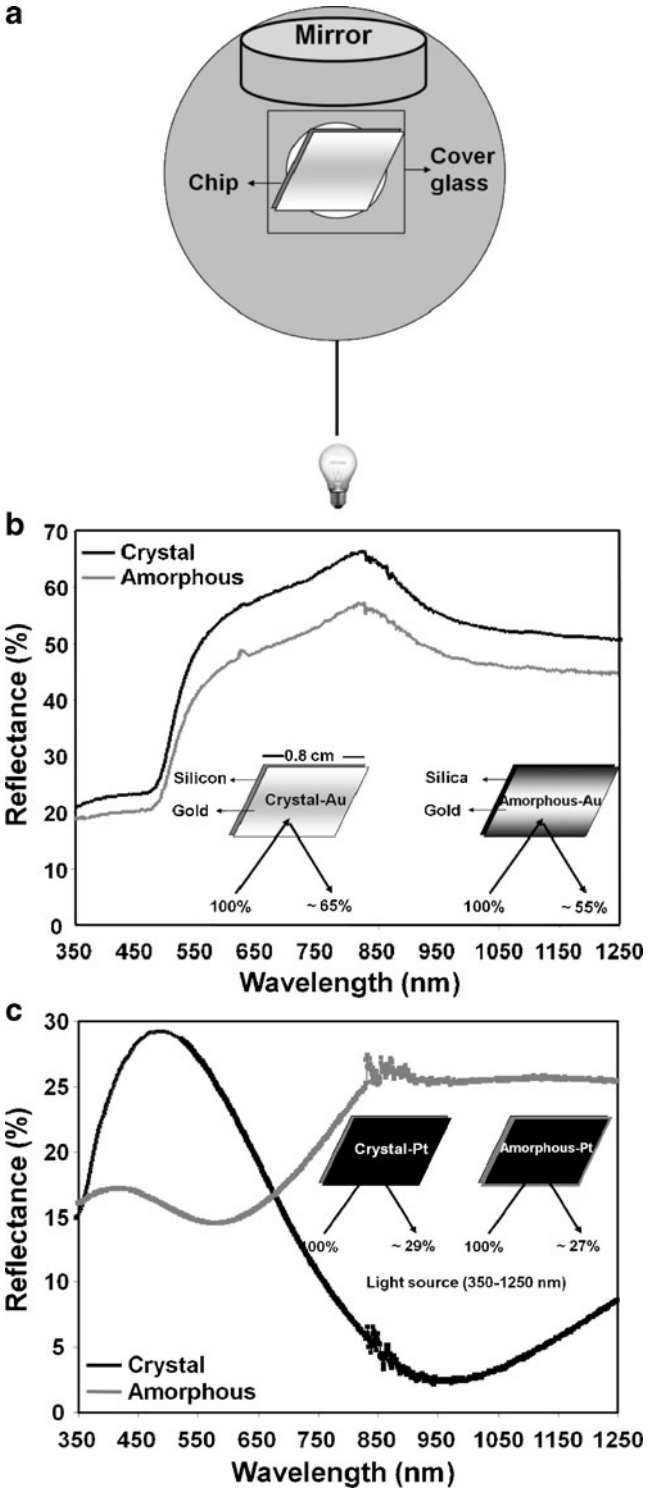

Fig. 1 **a** Set-up for the chip on a cover glass on the spectrophotometer. **b** Reflections measured on the spectrophotometer for gold-coated single-crystal silicon and glass chips at wavelengths from 350 to 1250 nm. Levels of reflections are as described in the text. **c** Reflections measured on the spectrophotometer for platinum coated single-crystal silicon and amorphous glass chips at wavelengths from 350 to 1250 nm. Levels of reflections are as described in the text

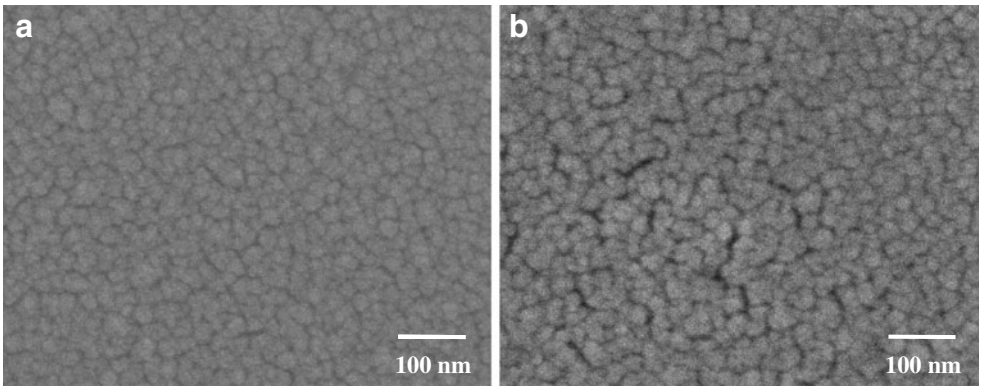

Fig. 2 Scanning electron microscopic images of the sensor chips' surface with **a** single-crystal silicon and **b** glass. A 100-nm thick Au layer was used in this case

than Au-coated materials and maximum reflectivity was observed in different wavelengths in both the cases of single-crystal silicon and amorphous glass. Based on these criteria, the present studies were continued with Au-coated materials as described below.

Effect of Au film thicknesses on the reflection

On the basis of the above results, we prepared single-crystal silicon substrates and deposited two Au films with thicknesses that differed by a factor of ten, namely 10 and 100 nm. After depositing the Au on silicon, we monitored the changes in reflectivity, as described above, over the range from 350 to 1250 nm. The substrates showed marked differences in their reflectivity. The substrate with the 10-nm Au film showed a maximum reflectivity of about 35%, whereas the substrate with the 100-nm Au film showed a reflectivity of 65% (Fig. 3a and b). These two Au layers showed about a twofold difference in reflectivity, indicating that there is a high probability of obtaining useful measurements by using a 100-nm-thick Au film.

The silicon substrates used in the present study were polished after slicing from grown ingot. Despite the polishing, it does not provide an atomically flat surface and still surface roughness occurs to some extent. When the gold is deposited onto the substrate surface, in the case of the thin layer (10 nm thick), the gold layer was not continuous and exhibited to some extent an island-like growth pattern. When the substrate was coated with thicker gold layer (100 nm thick), continued coating makes a smoother gold layer surface minimizing the island growth pattern by the continuous coat over the boundaries, along with the better adherence. This smooth surface of the thicker layer exhibited a higher reflectivity compared to the thinner gold layer. The difference in the reflectivity of these two layers is expected to be due to the distraction of light by the boundaries of the islands in the case of a 10-nm-thick film, which is absent in the case of 100 nm thick film. On the basis of these results, we went on to confirm the suitability of the 100-nm Au film for use in biosensors by analyzing DNA duplex formation, as described below.

Analysis of DNA duplex formation on crystalline chips

Because we were analyzing duplex formation on Au layers, we used a Au surface from Biacore as a reference. Specific duplex formation and the attachment of thiolated ssDNA (dT_{20}) were evaluated by means of SPR. Thiol molecules were attached on the 5′-end of DNA with 20 deoxythiamine

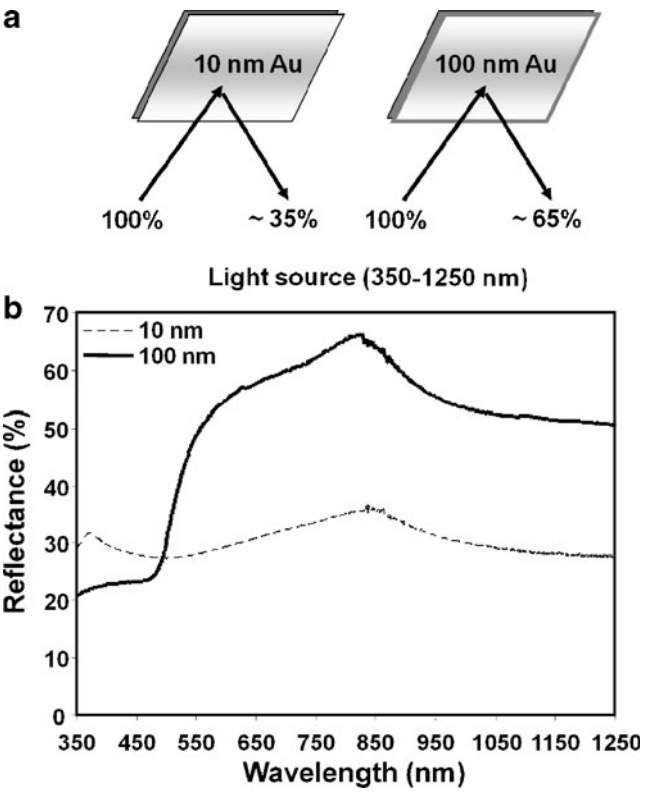

Fig. 3 **a** Reflectivities of single-crystal silicon coated with Au layers 10 and 100 nm thick. **b** Spectrophotometrically measured reflectivities of 10 and 100 nm thick layers of Au on single-crystal silicon at the wavelengths from 350 to 1250 nm

residues. SPR utilizes the oscillations of free charge at the interface between a dielectric medium and a surface that occur with small changes in the refractive index and the thickness of the dielectric layer. Variations in the spectral signals show the occurrence of biomolecular interactions at the interface. In the present study, the formation of a DNA duplex was tested by using Biacore 2000 with Au chips (Fig. 4a). As a control for the experiment, we injected noncomplementary DNA (dT_{20}) at the same concentration (1 μM) onto a Au surface with immobilized thiolated DNA (dT_{20}) with 1 μM, and we observed no change in the response. However, when we injected complementary DNA (dA_{20}), we observed a change in the response by about 300 response units at a similar concentration (1 μM) to that injected for the noncomplementary reaction, indicating the formation of a specific duplex on the Au surface.

We then carried out similar experiments on the Au films deposited on the single-crystal silicon substrate and

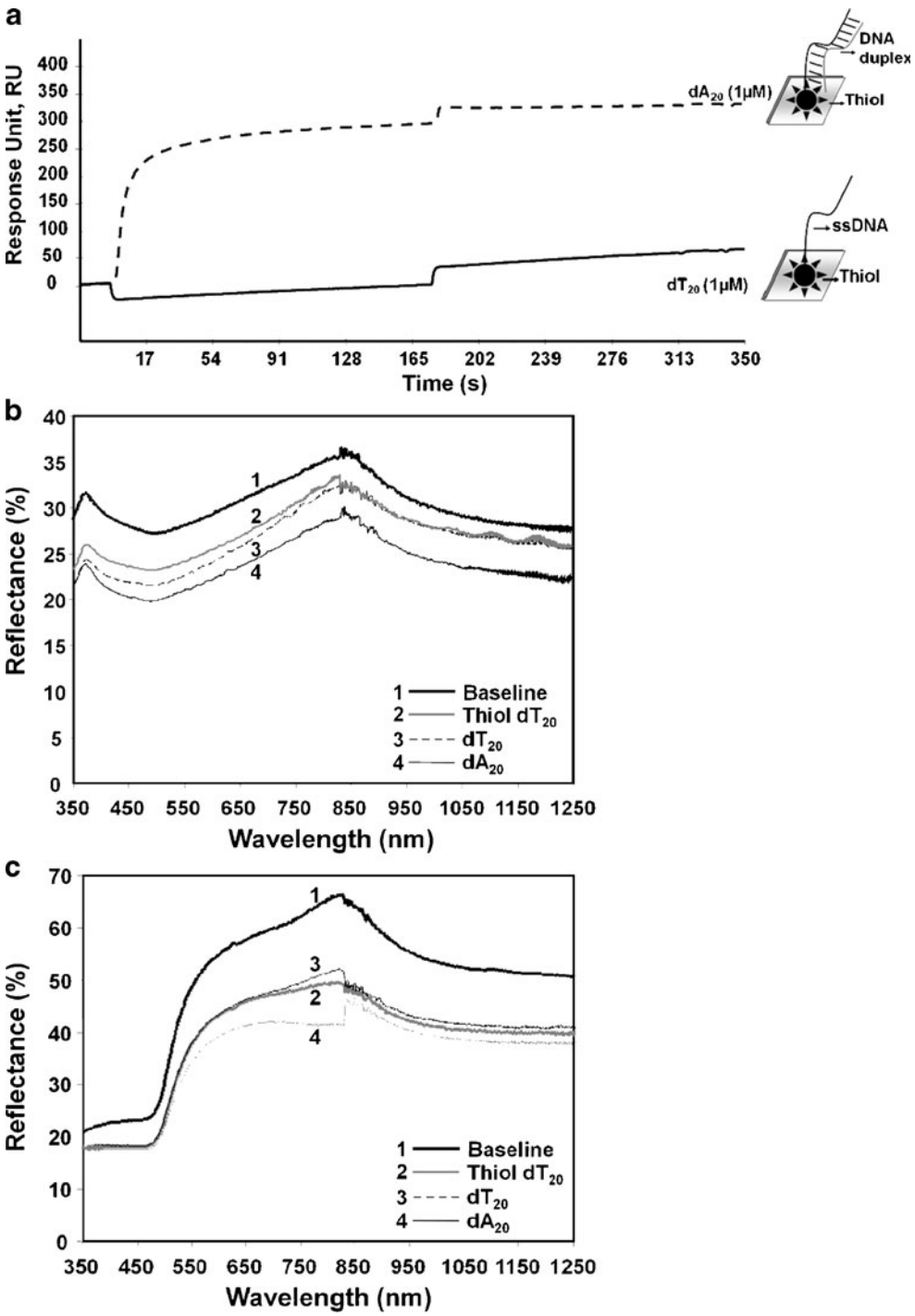

Fig. 4 **a** Specific binding with DNA duplex formation measured by the surface plasmon resonance. **b** Spectrophotometrically measured reflectivities of a single-crystal silicon chip with a 10 nm Au layer with attached DNA complexes measured at wavelengths between 350 and 1250 nm. Each DNA strand was used at a 1 μM concentration. dT_{20} was immobilized with a thiol, and the duplex was produced with dA_{20}. dT_{20} was injected as a negative control. **c** Spectrophotometrically measured reflectivities of a single-crystal silicon chip with a 100-nm Au layer with attached DNA complexes measured at wavelengths between 350 and 1250 nm

measured the reflectivity. We used both kinds of Au layers (10 and 100 nm) on which thiolated DNA (dT_{20}) with 1 μM was immobilized independently. As mentioned above, these thin Au films showed about a twofold difference in reflectivity in the absence of any biomolecules. Upon attaching the thiolated DNA (dT_{20}), the reflectivity decreased by 2% (from 35% to 33%) with the 10-nm Au film and by 15% (from 65% to 50%) with the 100-nm film. As expected, when noncomplementary DNA (dT_{20}) with 1 μM was added as a control, there was no significant change in the spectrum. When complementary DNA (dA_{20}) with 1 μM was added, however, a further decrease in reflectivity was observed; with the 10-nm Au film with the thiolated DNA the decrease was 3% (from 33% to 30%) whereas it was 10% (from 50% to 40%) in the case of the 100-nm film Au film with attached thiolated DNA (Fig. 4b and c, respectively). The small peak on the top edge of each spectrum arose because of the changes in the light source at 830 nm. Altogether, on the basis of reflectivity, the sensitivity appears to be higher with the 100-nm Au film than with the 10-nm Au film. However, a change was observed in both cases, and therefore, to reduce the cost of the film, a 10-nm layer can be used in the sensor, although the reflectivity is higher with the 100-nm Au film. The refractive index of the duplexed DNA (dT_{20} with dA_{20}) is 1.24, as measured by optical ellipsometry [11].

Analysis of aptamer-protein interactions on crystalline chips

To extend the above studies as the evidence for specific interactions, we performed the RNA-aptamer complementation on the DNA molecules and further analyses of the aptamer binding to the protein. We considered the previously reported high-affinity RNA-aptamer generated against human coagulating factor IX [19] for the present study. Aptamers (artificial ligands) are usually generated from randomized pool of molecules by repeated affinity and amplification processes [26]. Initially, the specific interactions of this aptamer (50 nM) and factor IX (100 nM) interactions were evaluated by Biacore-based surface plasmon resonance in the presence and absence of metal ions as they are necessary for specific interactions (Fig. 5a). These interactions were also evaluated with the present sensor chip with the buffer containing both calcium and magnesium ions. Before making the sensor surface with thiolated DNA molecules (dT_{20};1 μM), we tried to attach the same DNA molecules without thiol groups (dT_{20};1 μM) for specificity and we could not find any significant changes with non-specific attachments. With this evidence, we further attached the thiolated DNA strand and complemented with RNA-aptamer (1 μM; Electronic Supplementary Material figure S3). Upon attaching the

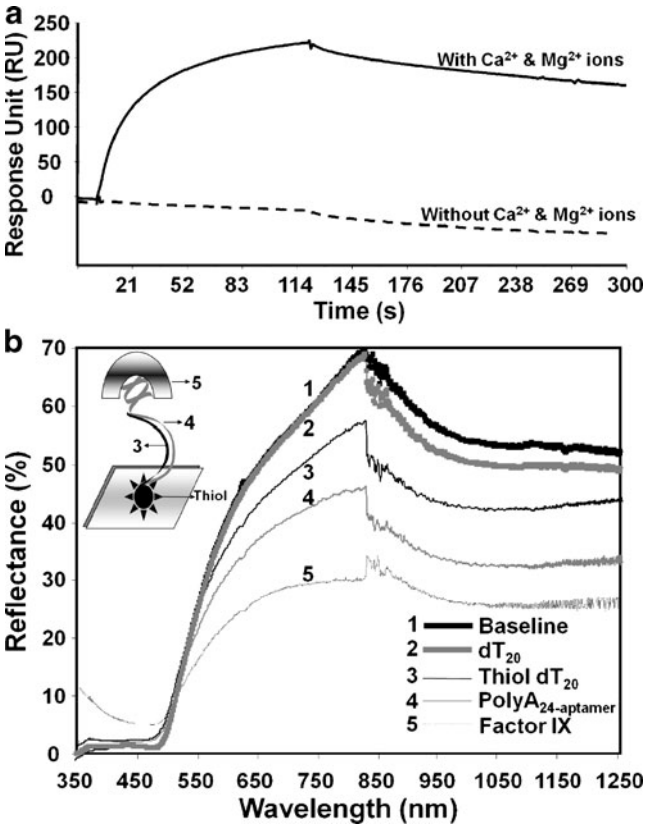

Fig. 5 **a** Specific binding for RNA-aptamer and protein interactions are measured by the surface plasmon resonance. **b** Spectrophotometrically measured reflectivities of a single-crystal silicon chip with a 100 nm Au layer with attached DNA–RNA aptamer followed by protein complexes measured at wavelengths between 350 and 1250 nm. Each nucleic acid strand was used at a 1 μM concentration. dT_{20} with 1 μM was immobilized without a thiol group at the first step for non-specific control

aptamer, we found the reflection changes about 10% (changes from 55% to 45%); by attaching the factor IX (100 nM), the change was about 12% (from 45 to 33%) as shown in the Fig. 5b, indicating the specific interactions of these molecules as evidenced by previous studies [10,19]. From these results, it is also evidenced that the sensor chip prepared in the present investigation can be used for the analyses of aptamer–ligand interactions with sub-nano molar concentration levels.

Based on the above evidence, the application spectrophotometric measurements as mentioned above can be applied for sensor developments. In addition, as reported by Chopra et al. [27], this method is simple, accurate, reproducible, selective, sensitive and cost effective. Chopra et al. [27] have performed spectrophotometric validation to estimate the trigonelline from polyherbal gels. Similarly, characterization of red mud by using UV–vis–NIR spectroscopy was performed [21]. At the advanced level, quantitative UV–visible spectroscopy analyses were performed for clinical and pre-clinical applications in cancer

[28]. Metal detection with trace amounts in fresh water sample by spectrophotometric methods was proposed to apply to deionized-, tap-, river-, lake- and reservoir- water samples as the important issues on environmental management [22]. A procedure was made spectrophotometrically to determine the copper using nitroso-R salt as chromogenic agent [24]. Clinical analysis on a lab-on-a-chip design for the measurements of biological fluids by spectrophotometric analysis was also shown in the past [23]. In addition several recent studies shows several other applications with spectrophotometer such as, biosensors for glucose determination [29], the colorimetric sensor [30], for the determination of anionic surfactants [31], dermatological studies [32] and for pharmaceutical preparation [33], as the broad applications.

Conclusion

The experiments preformed in the present study, clearly showed that a single crystal of silicon is a suitable substrate for making the sensor chips to monitor the biomomolecular interactions. Furthermore, the area of the Au film can be reduced by reducing the chip size through the use of a thin cover glass under the chip during analysis. Single-crystal silicon can be used as an alternative substrate in laboratories with fewer facilities and lower funding, to avoid the necessity of using expensive equipment. Further, as reported by Yu [34], the low-cost reflective gold layers can be made on the sensor chip described in this study with forming self-assembled monolayers. The results obtained in our studies will extend the range of methods available for the analysis of interactions of nucleic acids and ligands; in particular, the method is suitable for use with aptamer–small ligand interactions, as demonstrated in other sensor systems.

References

1. Guo P (2005) J Nanosc Nanotechnol 5:1964
2. Baldrich E, Restrepo A, O'Sullivan CK (2004) Anal Chem 76:7053–7063
3. Gronewold TMA, Glass S, Quandt E, Famulok M (2005) Biosens Bioelectron 20:2044–2052
4. Odenthal KJ, Gooding J (2007) Analyst (Cambridge, U K) 132:603–610
5. Marquette CA, Blum LJ (2008) Anal Bioanal Chem 390:155–168
6. Song S, Wang L, Li J, Zhao J, Fan C (2008) Trends Anal Chem 27:108–117
7. Varma MM, Nolte DD, Inerowicz HD, Regnier FE (2004) Opt Lett 29:950–952
8. Peng L, Varma MM, Cho W, Regnier FE, Nolte DD (2007) Appl Opt 46:5384–5395
9. Wang X, Zhao M, Nolte DD (2008) Appl Opt 47:2779–2789
10. Gopinath SCB, Awazu K, Kumar PKR, Tominaga J (2008) ACS Nano 2:1885–1895
11. Gopinath SCB, Awazu K, Fons P, Tominaga J, Kumar PKR (2009) Anal Chem (Washington, DC, U S) 81:4963–4970
12. Kumar P, Choithani J, Gupta KC (2004) Nucleic Acids Res 32:e80
13. Rong G, Najmaie A, Sipe JE, Weiss SM (2008) Biosens Bioelectron 23:1572–1576
14. Gonçalves D, Prazeres DMF, Chu V, Conde JP (2008) Biosens Bioelectron 24:545–551
15. Gopinath SCB, Awazu K, Fujimaki M, Sugimoto K, Ohki Y, Komatsubara T, Tominaga J, Gupta KC, Kumar PKR (2008) Anal Chem (Washington, DC, U S) 80:6602–6609
16. Gopinath SCB, Awazu K, Fujimaki M, Sugimoto K, Ohki Y, Komatsubara T, Tominaga J, Kumar PKR (2009) Anal Bioanal Chem 394:481–488
17. Sabate J, Anderson MA, Kikkawa H, Xu Q, Cervera-March S, Hill CG Jr (1992) J Catal 134:36–46
18. Ly SY, Lee JH (2009) Ann Biomed Eng 37:2028–2033
19. Rusconi CP, Scardino D, Layzer J, Pitoc GA, Ortel TL, Monroe D, Sullenger BA (2002) Nature 419:90–94
20. Kumaresan R, Umezawa H, Tatsumi N, Ikeda K, Shikata S (2009) Diam Relat Mater 18:299–302
21. Palmer SJ, Jagannadha Reddy B, Frost RL (2009) Spectrochim Acta Part A 71:1814–1818
22. Kawakubo S, Naito A, Fujihara A, Iwatsuki M (2004) Anal Sci 20:1159–1163
23. Minas G, Wolffenbuttel RF, Correia JH (2005) Lab Chip 5:1303–1309
24. Kruanetr S, Tengjaroenkul U, Liawruangrath B, Liawruangrath S (2008) Spectrochim Acta Part A 70:1134–1140
25. Clark ML, Green RL, Johnson OE, Fanwick PE, McMillion DR (2008) Inorg Chem 47:9410–9418
26. Gopinath SCB (2007) Anal Bioanal Chem 387:171–182
27. Chopra S, Motwani SK, Ahmad FJ, Khar RK (2007) Spectrochim Acta, Part A 68:516–522
28. Brown JQ, Vishwanath K, Palmer GM, Ramanujam N (2009) Curr Opin Biotechnol 20:1–13
29. Wu B, Zhang G, Shuang S, Choi MMF (2004) Talanta 64:546–553
30. Ercağ E, Üzer A, Apak R (2009) Talanta 78:772–780
31. El-Nemma EM, Badawi NM, Hassan SSM (2009) Talanta 78:723–729
32. Lister T, Wright P, Chappell P (2010) Lasers Med Sci 25:449–457
33. Zhang M, Zhang Y, Li Q (2010) Spectrochim Acta Part A 75:1013–1017
34. Yu H (2001) Anal Chem 73:4743–4747